Axon Terminals From the Nucleus Isthmi Pars Parvocellularis Control the Ascending Retinotectofugal Output Through Direct Synaptic Contact With Tectal Ganglion Cell Dendrites

Cristian González-Cabrera,[1] Florencia Garrido-Charad,[1] Jorge Mpodozis,[1] J. Paul Bolam,[2] and Gonzalo J. Marín[1,3]*

[1]Departamento de Biología, Facultad de Ciencias, Universidad de Chile, Santiago, Región Metropolitana, Chile
[2]Medical Research Council Anatomical Neuropharmacology Unit, Department of Pharmacology, University of Oxford, Oxford OX1 2JA, United Kingdom
[3]Facultad de Medicina, Universidad Finis Terrae, Providencia, Santiago, Región Metropolitana, Chile

ABSTRACT

The optic tectum in birds and its homologue the superior colliculus in mammals both send major bilateral, nontopographic projections to the nucleus rotundus and caudal pulvinar, respectively. These projections originate from widefield tectal ganglion cells (TGCs) located in layer 13 in the avian tectum and in the lower superficial layers in the mammalian colliculus. The TGCs characteristically have monostratified arrays of brush-like dendritic terminations and respond mostly to bidimensional motion or looming features. In birds, this TGC-mediated tectofugal output is controlled by feedback signals from the nucleus isthmi pars parvocellularis (Ipc). The Ipc neurons display topographically organized axons that densely ramify in restricted columnar terminal fields overlapping various neural elements that could mediate this tectofugal control, including the retinal terminals and the TGC dendrites themselves. Whether the Ipc axons make synaptic contact with these or other tectal neural elements remains undetermined. We double labeled Ipc axons and their presumptive postsynaptic targets in the tectum of chickens (*Gallus gallus*) with neural tracers and performed an ultrastructural analysis. We found that the Ipc terminal boutons form glomerulus-like structures in the superficial and intermediate tectal layers, establishing asymmetric synapses with several dendritic profiles. In these glomeruli, at least two of the postsynaptic dendrites originated from TGCs. We also found synaptic contacts between retinal terminals and TGC dendrites. These findings suggest that, in birds, Ipc axons control the ascending tectal outflow of retinal signals through direct synaptic contacts with the TGCs. J. Comp. Neurol. 524:362–379, 2016.

INDEXING TERMS: optic tectum; superior colliculus; attention; stimulus selection; vision; ultrastructure; RRID:AB_2336654; RRID:AB_10013220; RRID:AB_2336126; RRID:nif-0000-23420

The optic tectum (TeO), or superior colliculus (SC) in mammals, is the main extrageniculate visuomotor center in all vertebrates, mediating eye and head orientation, avoidance reactions, stimulus selection, visual discriminative behaviors, and spatial attention (Ingle, 1983; Wylie et al., 2009; Gandhi and Katnani, 2011; Comoli et al., 2012; Krauzlis et al., 2013). The tectum sends several projections to the thalamus, one of which is bilateral and nontopographic and directed specifically to the nucleus rotundus (Rt) in birds (Benowitz and Karten, 1976) and to the caudal pulvinar in mammals (Luppino et al., 1988; Lyon et al., 2003; Day-Brown et al., 2010; Baldwin et al., 2011; Fredes et al., 2012). This projection arises exclusively from tectal ganglion cells (TGCs), located in layer 13 of the avian TeO

Grant sponsor: FONDECYT; Grant number: 1110281 (to G.J.M); Grant number: 1151432 (to G.J.M); Grant sponsor: Medical Research Council of the United Kingdom (to J.P.B.).

J. Paul Bolam is now at MRC Brain Network Dynamics Unit, Department of Pharmacology, University of Oxford, Oxford, United Kingdom.

*CORRESPONDENCE TO: Cristian González-Cabrera and Gonzalo J. Marín Gamé, Las Palmeras 3425, Ñuñoa, Santiago, 7800003 Chile. E-mail: cristian.gonzalez.ca@gmail.com and gmarin@uchile.cl

Received May 25, 2015; Revised July 10, 2015;
Accepted July 24, 2015.
DOI 10.1002/cne.23860
Published online August 18, 2015 in Wiley Online Library (wileyonlinelibrary.com)

(Karten et al., 1997; Marín et al., 2003) and in the lower stratum griseum superficialis and upper stratum opticum layers of the mammalian SC (Robson and Hall, 1977; Major et al., 2000; Chomsung et al., 2008; Fredes et al., 2012; Gale and Murphy, 2014). The TGCs exhibit an evolutionarily conserved widefield morphology, featuring monostratified arrays of brush-like dendritic terminations (bottlebrushes), whose layer allocation varies with the TGC type (Luksch et al., 1998, 2001; Major et al., 2000; Hellmann and Güntürkün, 2001; May, 2006). Recordings in avian (Schmidt and Bischof, 2001; Wu et al., 2005) and mammalian (Humphrey, 1968; Gale and Murphy, 2014) species have shown that TGCs respond to bidimensional motion of small objects or to looming stimuli and, thus, mainly convey visual motion signals to the thalamus and thence to the pallium.

Although the functional significance of the TGC-mediated tectofugal pathway is unclear, its visual output in birds is prominently controlled by the isthmotectal network (Marín et al., 2007, 2012). This network is similarly organized across vertebrate classes, and substantial evidence suggests that it plays a role in target selection and spatial attention (Sereno and Ulinski, 1987; Gruberg et al., 2006; Marín et al., 2007, 2012; Mysore and Knudsen, 2011; Sridharan and Knudsen, 2014). In birds, the isthmic control is effected by the nucleus isthmi pars parvocellularis (Ipc), which receives topographically organized visual inputs from "shepherd's crook" neurons located in tectal layer 10 and feeds back space-specific signals to the same tectal locus (Hunt et al., 1977; Güntürkün and Remy, 1990; Marín et al., 2005; Wang et al., 2006). This feedback is mediated by brush-like columnar axon terminals, which overlap in the superficial and intermediate tectal layers with several structures involved in the TGC visual responses, such as the retinal axon terminals, the shepherd's crook neurons, and the TGC dendritic terminals themselves. Preventing this feedback in a given tectal locus eliminates visual responses in the Rt from the corresponding location of visual space, suggesting a causal interaction between the Ipc feedback and the TGC visual output (Marín et al., 2007, 2012).

To define the anatomical basis of the Ipc control over TGCs in birds, we double labeled Ipc axons and their presumptive postsynaptic targets in the TeO of chickens (*Gallus gallus*) with neural tracers and performed an ultrastructural analysis of serial sections of the TeO. Our results indicate that direct synaptic contacts within glomerulus-like structures between Ipc axonal boutons and TGC dendrites are the structural basis underlying the strong control exerted by the Ipc on the visual outflow of the TGCs.

MATERIALS AND METHODS

Animals

Experiments were conducted on 11 broiler chickens (*Gallus gallus domesticus*; U.S. National Center for Biotechnology Information taxonomy ID: 9031) of both sexes, obtained from a local dealer and maintained in an institutional facility. The ages of the animals ranged from 12 to 16 weeks. All procedures were approved by the Ethics Committee of the Science Faculty of the University of Chile and conformed to the guidelines of the National Institutes of Health on the use of animals in experimental research.

In vivo neural tracer injections

To investigate the synaptic targets of the Ipc axon terminals, four types of experiments were performed. First, cholera toxin subunit B (CTb) injections were administered to one eye to label the retinal terminals in the contralateral TeO (n = 2). Second, injections of the anterograde tracer *Phaseolus vulgaris* leucoagglutinin (PHA-L) were administered to the Ipc to label the axon terminals in the TeO (n = 3). Third, injections of PHA-L were administered to the Ipc, combined with biotinylated dextran amine (BDA) 3k in the Rt (n = 3) to label the TGCs retrogradely in the TeO. Fourth, injections of BDA 3k were administered in the Ipc (n = 3) to label the shepherd's crook neurons retrogradely and to label the Ipc terminals anterogradely in the TeO.

For the intraocular CTb injection experiments, the birds were sedated and anesthetized with a mixture of 4% halothane in oxygen, delivered at a constant flow of 1 liter/minute with a customized mask placed around the bill. The skin dorsal to the eye was incised with a scalpel to expose the eyeball. A small cut was made in the dorsal sclera, through which 20 μl of 0.8% CTb in phosphate-buffered saline (PBS; 0.01 M phosphate buffer, pH 7.4, 0.876% NaCl) with 2% dimethylsulfoxide (DMSO; List Biological Laboratories, Campbell, CA) was injected into the eye's vitreous body with a Hamilton syringe (Hamilton Company, Reno, NV). After the procedure, the skin wound was closed with instant adhesive and treated with antiseptic povidone–iodine solution.

For the single and double injections of neural tracers in the Ipc and the Rt, chickens were anesthetized by an intramuscular injection of ketamine/xylazine mixture (ketamine 75 mg/kg, xylazine 5 mg/kg) and placed in a stereotaxic frame that did not interfere with the animal's visual field. Depending on the experiment type, one or two small windows were opened on the right

TABLE 1.
Primary Antibodies Used

Antigen	Description of immunogen	Source, host species, catalog No., RRID	Concentration used
PHA-L	Pure lectins	Vector Laboratories, biotinylated goat anti-PHA-L, B-1115, AB_2336654	Dilution 1:5,000
CTb	CTb	List Biological Laboratories, goat anti-CTb; 703, AB_10013220	Dilution 1:40,000

side of the skull, exposing the dorsolateral part of the tectum above the isthmi and the telencephalic region overlying the Rt (anterior, 6.5–7.0 mm from the interaural canal; lateral, 2.5 mm from the midline). To identify the lpc and the Rt nuclei, exploratory extracellular recordings were performed in the tectal and thalamic areas with tungsten electrodes (1 MOhm; FHC, Bowdoin, ME) and a conventional recording system. Hand-held objects and a laser pointer were used as visual stimuli. The lpc neurons show strong bursting responses to moving stimuli presented in their 15–20° receptive fields (RFs; Marín et al., 2005). The Rt displays characteristic multiunit responses to small moving stimuli from large RFs that cover most part of the visual field. After the respective nucleus was localized, in the case of the lpc, the tungsten electrode was replaced by a micropipette (10–15-μm tip) loaded with the tracer PHA-L (2.5% PHA-L in 10 mM phosphate buffer, pH 8; Vector Laboratories, Burlingame, CA) or BDA 3k (10% in 0.1 M phosphate buffer, pH 8; Invitrogen, Eugene, OR); in the case of the Rt, the tungsten electrode was replaced by a micropipette (25–30-μm tip) loaded with BDA 3k solution (same as described above). All injections were made by iontophoresis with 7 μA of positive current for 35 minutes and a 7-seconds-on/7-seconds-off duty cycle (Stoelting, Wood Dale, IL).

Tissue preparation for electron microscopy

After 7–10 days, the chickens were deeply anesthetized with ketamine/xylazine solution and perfused with 200 ml PBS (0.01 M phosphate buffer, pH 7.4, 0.876% NaCl, 0.02% KCl), followed by 160 ml fixative solution (3% paraformaldehyde, 0.1% glutaraldehyde, 0.1 M PB, pH 7.4). The brains were removed, postfixed for 1 hour in the same fixative, and cut into 80-μm coronal sections with a Vibratome (VT1000S; Leica Microsystems, Wetzlar, Germany). The sections were incubated in a cryoprotectant solution (10% glycerol, 25% sucrose in PB 0.1 M) for 2 hours, placed flat on the bottom of a plastic dish, and then freeze–thawed twice by floating in liquid nitrogen.

Histochemistry and immunohistochemistry

For single-label procedures, sections were incubated with the appropriate reagents overnight and then the injected tracers were revealed by a peroxidase method with diaminobenzidine (DAB) as the chromogen. In the case of CTb immunohistochemistry, the sections were immersed in 10% methanol/3% H_2O_2 for 10 minutes to quench endogenous peroxidase activity and incubated overnight with a primary polyclonal anti-CTb antibody (anti-CTb goat antibody; catalog No. 703; RRID:AB_10013220; List Biological Laboratories; diluted 1:40,000 in PBS/0.3% Triton X-100/3% normal rabbit serum; Table 1). After having been washed in PBS, the sections were incubated for 1 hour with a biotinylated rabbit anti-goat antibody (anti-goat rabbit antibody IgG (H+L); catalog No. BA-5000; RRID:AB_2336126; Vector Laboratories; diluted 1:1,000 in PBS/0.3% Triton X-100), and then, after additional washes, in ABC solution (avidin–biotin–peroxidase complex; Vectastain Elite ABC kit; Vector Laboratories) to bind to the biotinylated secondary antibodies. In a final step, the peroxidase reaction was performed with DAB as the chromogen by incubating the sections for 10 minutes in a 0.025% DAB solution in Tris buffer (pH 8) and reacted by adding hydrogen peroxide solution (0.0025% H_2O_2 solution, final concentration). In the case of the PHA-L injections, the sections were incubated overnight with biotinylated anti-PHA-L antibody (biotinylated goat anti-PHA-L; catalog No. B-1115; RRID:AB_2336654; Vector Laboratories; diluted 1:5,000 in blocking solution of 3% normal donkey serum in PBS; Table 1). The sections were then washed three times in PBS, incubated in ABC for 90 minutes, and revealed by the peroxidase/DAB reaction, as described above. Sections from single BDA injections were incubated in ABC solution, washed three times in PBS, and then revealed by peroxidase/nickel-DAB (Ni-DAB) reaction.

For double labeling with BDA and PHA-L, the tracers were revealed sequentially. First, sections were incubated in ABC solution for 90 minutes, and the BDA was revealed with the peroxidase/Ni-DAB reaction (0.33% nickel ammonium sulfate included in the reaction mixture). After three washes in PBS, the sections were placed in blocking solution for 1 hour and then incubated overnight with biotinylated anti-PHA-L antibody at a dilution of 1:5,000 in blocking solution. After three washes in PBS, the sections were reincubated in ABC for 90 minutes and then revealed with the peroxidase/DAB reaction.

After three washes in PBS and two washes in PB, sections were placed flat on the bottom of a Petri dish and fixed with osmium tetroxide (1% in PB; Oxkem, Oxford, United Kingdom) for 40 minutes. Sections were then washed three times in PB and dehydrated in an ascending series of ethanol dilutions (15 minutes in 50% ethanol, 40 minutes in 75% ethanol and 1% uranyl acetate [TAAB, Reading, United Kingdom], 15 minutes in 95% ethanol, and two steps of 15 minutes each in absolute ethanol). Sections were exposed twice to propylene oxide (Sigma-Aldrich, St. Louis, MO) for 15 minutes and then immersed in resin (Durcupan; Fluka, Gillingham, United Kingdom) in plastic containers and left overnight at room temperature. On the following day, resin was gently warmed to reduce viscosity, and sections were transferred to microscope slides. A coverslip was applied, and the resin was cured at 65°C for 48 hours.

Electron microscopic analysis

Resin-embedded sections were examined in the light microscope, and the tectal areas of interest were selected on the basis of the presence of single- or double-labeled neural elements. These areas were photographed (under ×10 and ×40 objectives), cut from the slide, glued to the top of premade resin cylinders, and trimmed with a razor blade. Ultrathin serial sections, ~50-nm thick (silver/gray), were then cut with an ultramicrotome (Leica EM UC6; Leica Microsystems, Buffalo Grove, IL) and collected on pioloform, single-slot copper grids (Agar Scientific, Stansted, United Kingdom). To facilitate the identification of tectal layers, all preparations were cut while keeping the tectal layer 1 as a radial reference. To improve contrast for electron microscopic (EM) examination, the sections were lead stained. Serial sections were examined with a Philips CM10 or CM100 electron microscope. Although all tectal layers were examined, most of the analysis was centered on tectal layers 2–4, 5, 9, and 10, which contain a higher density of Ipc terminals.

To assess whether the Ipc terminal boutons (glomeruli) made synaptic contact with the apposed dendritic elements, a synaptic analysis of selected glomeruli was performed with micrographs of ultrathin serial sections (50–60 consecutive sections analyzed per animal, n = 3) of PHA-L single-labeled sections. Apposed dendritic profiles and postsynaptic densities in these dendrites were counted in every consecutive section (bouton/glomeruli from layers 2–4, n = 10; layer 5, n = 15; layer 9, n = 9).

To make three-dimensional (3D) reconstructions of selected Ipc terminal segments containing several bouton/glomeruli, the corresponding EM profiles were followed through their whole extent by using aligned consecutive micrographs. Alignment and 3D reconstructions were performed in the free access software Reconstruct (Synapse Web; RRID:nif-0000-23420; http://synapses.clm.utexas.edu/tools/reconstruct/reconstruct.stm).

TABLE 2.
EM and Brightfield Volumes of Ipc Axon Terminal Boutons in the TeO

TeO	Volume A[1] (μm³)	Volume B[2] (μm³)
Layers 2 and 3	0.72 ± 0.16	1.07 ± 0.16
Layer 5	1.79 ± 0.65	1.14 ± 0.12
Layer 9	0.54 ± 0.28	0.49 ± 0.08

[1]EM.
[2]Brightfield microscopy.

To assess further whether the glomeruli/bouton terminal structures reconstructed at the EM level and the bouton-like structures observed in light microscopy (LM) were indeed the same, we compared the estimated volumes in each case. Volumes of structures identified in the electron microscope were calculated by multiplying the area of the labeled profiles by the thickness of the section, adding this product in consecutive ultrathin sections of complete Ipc glomeruli (layers 2–4, n = 5; layer 5, n = 4; layer 9, n = 5; Table 2). LM volumes were analyzed in equivalent embedded sections (n = 3) at different tectal levels (layers 2–4, n = 122; layer 5, n = 151; layer 9, n = 62). Because the boutons were too small and normal stereological methods were impractical at ×100, we measured the long and transverse diameters of each bouton and calculated the volume of the corresponding solid of revolution (Table 2). EM and LM measurements were performed in Reconstruct and ImageJ, respectively. No account was taken for shrinkage of the tissue.

RESULTS

Ultrastructural characterization of the Ipc axon terminals

The Ipc axons reach the tectum following tectal layer 14 and bend upward toward the superficial layers, forming columnar brush-like arborizations (35–50 μm wide) from layers 2 to 10. The vertical branches ramify profusely, giving off very thin branches loaded with rounded boutons, which are extremely dense in layer 5 and less dense but still conspicuous in layers 2–4 and 8–10 (Wang et al., 2006).

Local injections of PHA-L into the Ipc led to the strong labeling of groups of Ipc axon terminals in the TeO throughout their radial extensions (Fig. 1A,B). The individual thin branches were beaded with rounded boutons and were clearly visible at high magnification by

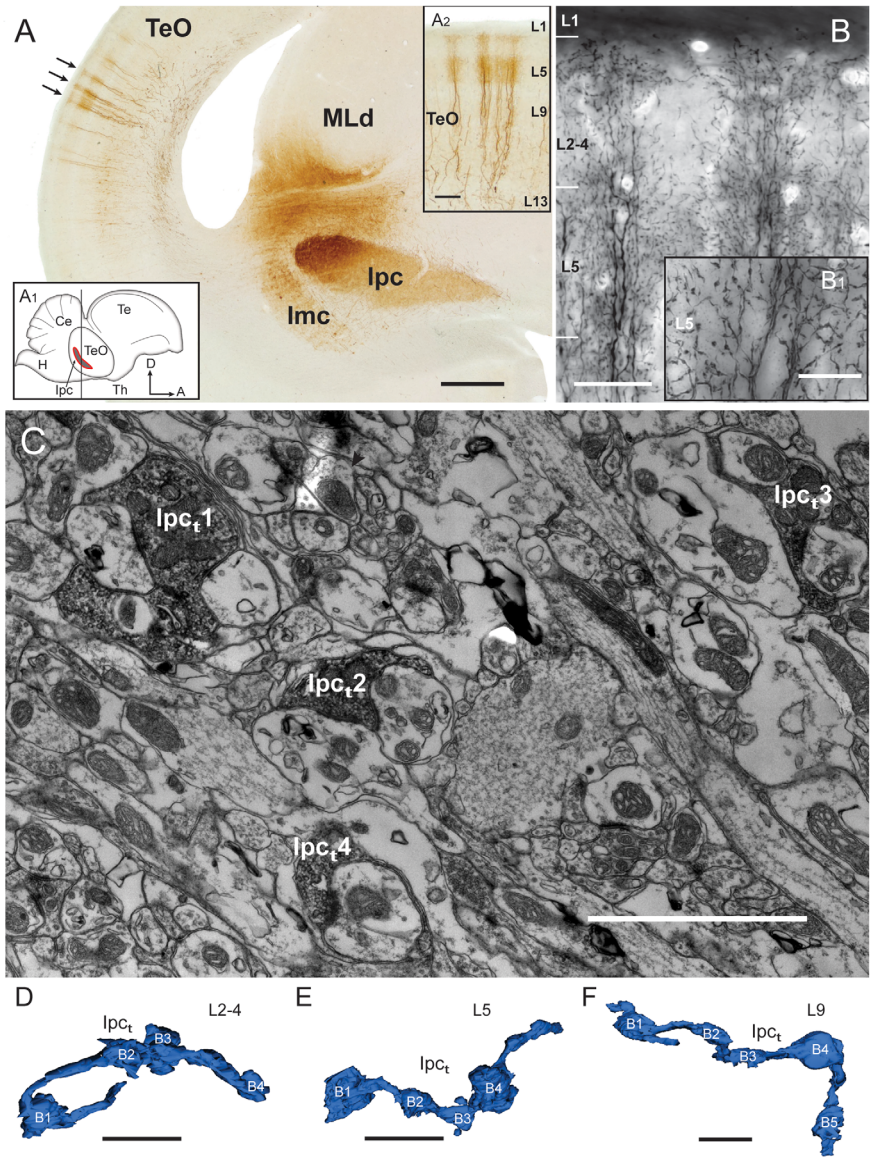

Figure 1. Ultrastructure of the Ipc axon terminals. **A:** Low-magnification micrograph of a coronal section (**A_1**) shows a PHA-L injection into the nucleus Ipc and anterogradely labeled axon terminals (black arrows) in the TeO (**A_2**). **B:** Light micrograph of a resin-embedded section with PHA-L labeled Ipc axon terminals in the TeO. High-magnification micrograph (**B_1**) shows the characteristic appearance of Ipc axonal boutons. **C:** Low-magnification electron micrograph of an ultrathin section obtained from layer 5 of the same sample shown in B. The anterogradely labeled Ipc axon terminals (four of which are visible in this field, Ipc_{t1-4}) are identified by the electron-dense peroxidase reaction product formed by the DAB. **D–F:** 3D reconstruction of PHA-L-labeled Ipc terminal segments obtained from EM serial sections in tectal layers 2–4 (D), 5 (E), and 9 (F). Note the thin fibers with interspersed boutons (B1–B5) producing the characteristic beaded appearance observed in brightfield microscopy (B_1). A, anterior; Ce, cerebellum; D, dorsal; H, hindbrain; Imc, nucleus isthmi pars magnocellularis; MLd, nucleus mesencephalicus lateralis, pars dorsalis; Te, telencephalon; Th, thalamus. Scale bars = 500 μm in A; 100 μm in A_2; 50 μm in B; 20 μm in B_1; 2 μm in C–F. [Color figure can be viewed in the online issue, which is available at wileyonlinelibrary.com.]

brightfield microscopy (LM; Fig. 1B). After re-embedding and ultrathin sectioning (50 nm), the same tissue was examined in the electron microscope and revealed numerous DAB-labeled terminal profiles with an irregular, rounded shape and packed with synaptic vesicles. These labeled profiles were especially common in layer 5, in which three to five could be observed within a single low-power field (Fig. 1C). The rounded appearance, spatial configuration, and layer distribution of these profiles suggested that they correspond specifically to the rounded boutons of the Ipc axon terminals (Fig. 1A,B).

To be certain of the morphological equivalence of these DAB-labeled profiles, we measured their volume at both the EM (3D reconstructions of 50–60 serial sections, n = 14; Table 2; see Materials and Methods) and LM (n = 334) levels. There were no significant

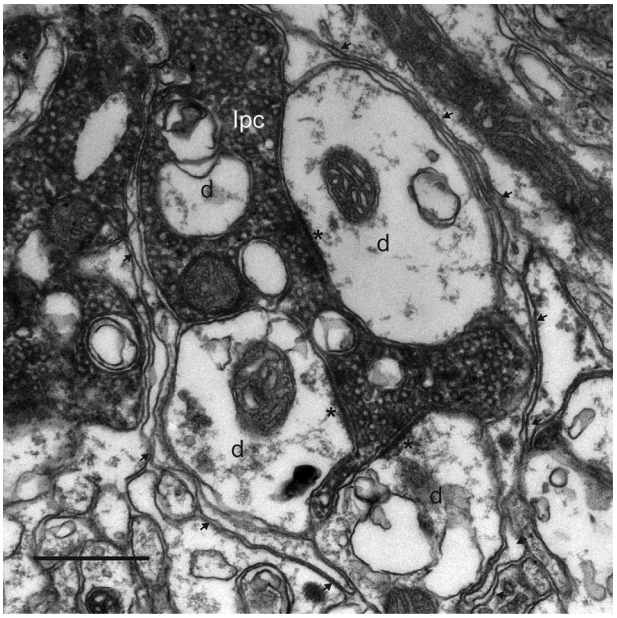

Figure 2. Ipc axon terminal boutons are organized into glomerulus-like structures. An electron micrograph shows an anterogradely labeled Ipc bouton in apposition to several dendritic profiles (d). Both the Ipc bouton and the dendrites are surrounded by glial membrane (arrows). This micrograph shows that the Ipc bouton establishes asymmetrical synapses (type I; asterisks) with three dendritic profiles included in the glomerulus. Scale bar = 0.5 μm.

differences between them (two-way ANOVA, $P = 0.57$). The EM and LM data also gave rise to equivalent values across layers. Thus, although the average volumes of boutons and profiles in tectal layers 2–4 and 5 were not significantly different (ANOVA, $P = 0.24$), they were larger than those measured in layer 9 (ANOVA, Holm-Sidak multiple-comparisons test, $P < 0.0001$; Table 2).

A final confirmation of this equivalence came from serial reconstructions (30–60 consecutive sections) of short segments of DAB-labeled terminal profiles in the superficial layers 2–4 and 5 as well as in the deeper layer 9, which revealed the characteristic morphology of the thin terminal fibers, beaded with rounded thickenings (Fig. 1D–F). These labeled terminals established asymmetrical (type I) synapses with several dendritic profiles (Fig. 2). They were bounded by glial membrane forming a glomerulus-like structure, similar to the "nonretinal glomeruli" previously described for the retinorecipient tectal layers of the pigeon (Hayes and Webster, 1975; Angaut and Repérant, 1976). This characteristic glomerular morphology was more evident in tectal layers 2–4 and 5 than in deeper layers (7–10), although in the deeper layers the labeled presynaptic profiles still established asymmetric synapses with two or three dendritic profiles (see below). These results show that Ipc boutons are indeed presynaptic structures, establishing synaptic contact with multiple dendritic profiles in superficial and deep tectal layers and forming complex, glomerular-like structures in the superficial layers.

Identification of Ipc synaptic targets

Neural tracers and EM

As mentioned in the introductory paragraphs, Ipc activity has been shown to exert a strong control over the tectofugal visual flow (Marín et al., 2007, 2012). Because the visual flow of this pathway is mediated by the TGCs, the dendritic specializations that codistribute with the Ipc axon terminals in the superior and deep tectal layers (Luksch et al., 1998, 2001; Hellmann and Güntürkün, 2001; Wang et al., 2006), we designated these cells as possible synaptic targets of the Ipc terminals.

Tectal layer 5 (TGCs I_{5a}–I_{5b})

Double injections of PHA-L and BDA 3k in the Ipc and Rt nuclei, respectively (Fig. 3A), resulted in anterogradely labeled Ipc axon terminals and retrogradely labeled dendritic structures (bottlebrushes) of the type I TGCs, which were especially dense in tectal sublayers 5a and 5b (Fig. 3B,C). The selected zone for the EM analysis of one representative case is shown in Figure 3C.

As was observed in the single-labeled material, low-magnification analysis of tectal layer 5 in the electron microscope revealed many labeled Ipc boutons within a single field. The same field often contained BDA-labeled profiles corresponding to retrogradely labeled TGC dendritic structures (Fig. 4A), in which five boutons are present in a single micrograph, three of which were apposed by BDA-labeled TGC dendrites. PHA-L-labeled profiles were distinguished from retrogradely BDA-labeled structures by the strong electron density of DAB deposits compared with the more floccular Ni-DAB precipitates. The identification of cellular structures was based on the descriptions of Peters et al. (1991). Profiles were identified as axons by the presence of numerous presynaptic vesicles. Dendrites were defined by the presence of postsynaptic densities and endoplasmic reticulum. Higher magnification revealed that, in these double-labeled sections, the glomerular structures formed by the Ipc bouton contacted up to two labeled TGC dendritic profiles (Fig. 4C,D). Normally the Ni-DAB reaction product that filled the TGC dendrites precluded the distinction of postsynaptic densities (Fig. 4B,C); however, in cases in which the profiles contained less reaction product, the synaptic densities were evident (Fig. 4D). All the unlabeled and Ni-DAB-labeled

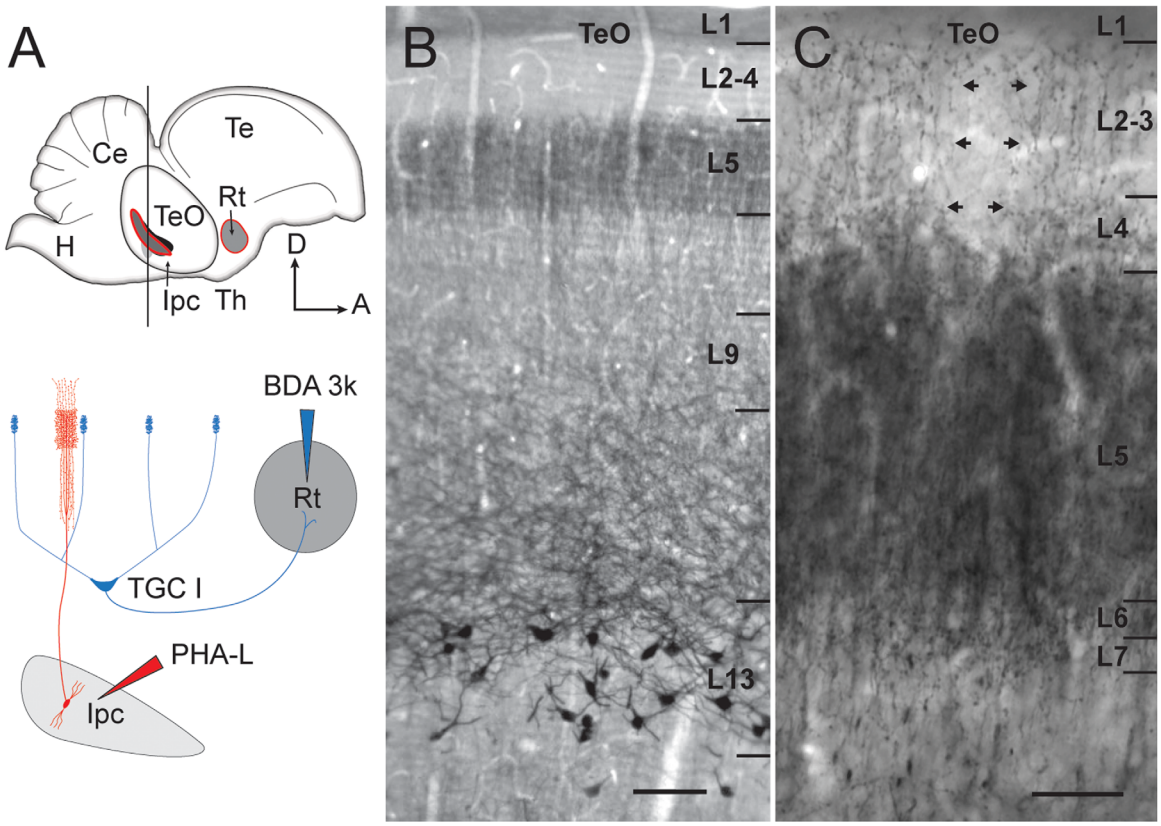

Figure 3. Double labeling of TGCs and Ipc terminals. **A:** Diagram of the Ipc and Rt nuclei in the chicken brain and the injections performed to label the cell bodies and dendrites of TGCs retrogradely and to label Ipc axons anterogradely. **B:** Light micrograph of a resin-embedded midbrain coronal section shows Ni-DAB-labeled TGC cell bodies in layer 13 and a dense band of bottlebrushes in layer 5. **C:** Enlarged view of the same sample shows labeled Ipc axon terminals (arrows) extending up to layers 2 and 3. A, anterior; BDA 3k, biotinylated dextran amine 3,000 Da; Ce, cerebellum; D, dorsal; H, hindbrain; Te, telencephalon; Th, thalamus. Scale bars = 100 μm in B; 50 μm in C. [Color figure can be viewed in the online issue, which is available at wileyonlinelibrary.com.]

profiles observed in close apposition with the Ipc boutons forming the glomeruli were identified as dendrites. Occasionally, some unlabeled neurites containing vesicles were observed postsynaptic to the Ipc axons, but whether they were dendrites or axons could not be determined.

Three-dimensional reconstruction of three connected glomeruli was performed with 38 consecutive ultrathin sections (50 nm) obtained from an experiment with a single injection in the Ipc (Fig. 4E,F). This revealed that most of the dendrites contacting the glomeruli formed knob-like structures that terminated inside the glomerulus, some of which might correspond to the tips of the hair-like dendritic specializations that form the bottlebrushes of the TGCs. On the other hand, a reconstruction of another Ipc terminal segment, with four connected glomeruli and labeled TGCs, showed that some TGCs made synapses "en passant" with the glomeruli through knob-like thickenings of the TGC dendritic processes (e.g., TGCs 1 and 3; Fig. 4G–J). These results show that the Ipc axon boutons make frequent synaptic contacts with dendritic specializations of the type I_{5a} and type I_{5b} TGCs.

Tectal layers 2–4 (TGCs I_{2-4})

In the same double-labeled material, retrogradely labeled bottlebrushes were also scattered in tectal sublayers 2–4 (Fig. 5B,C). EM analysis revealed glomerular structures similar to those found in layer 5 (Fig. 5B,C) but with fewer dendritic profiles (two or three per glomerulus). As in layer 5, in the double-labeled tissue, close appositions were found between Ipc boutons and type I_{2-4} TGC dendrites (Fig. 5B,C). Also, although the Ni-DAB reaction product made it difficult to identify the postsynaptic specializations, in some less densely labeled cases clear postsynaptic densities were evident (Fig. 5C).

Three-dimensional reconstruction (57 sections) of four connected labeled Ipc boutons was performed in single-labeled tissue (Fig. 5D,E). This reconstruction showed that, as in layer 5, some of the dendrites contacting the Ipc bouton formed knob-like structures that terminated inside the glomerulus and might correspond

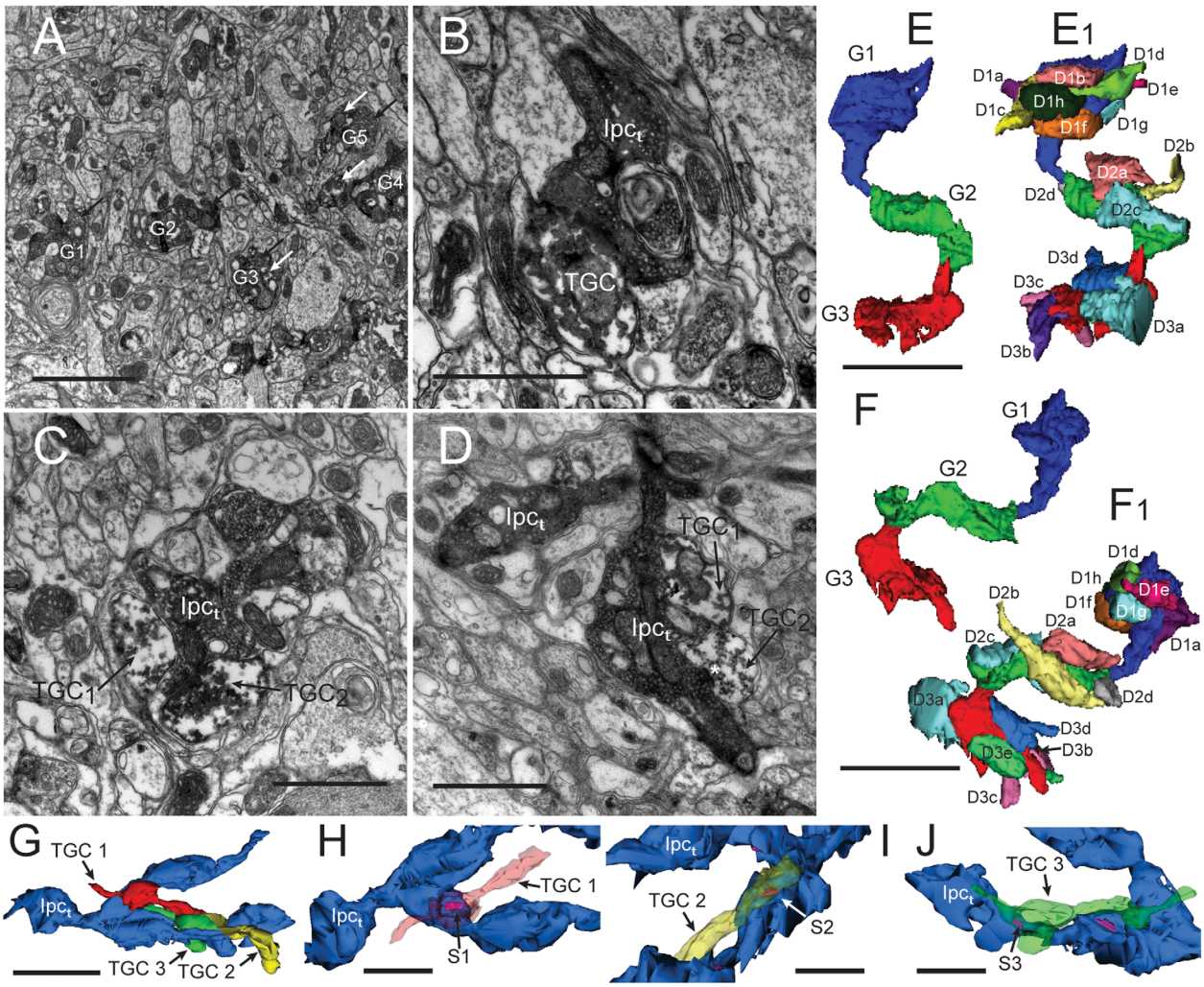

Figure 4. Ipc boutons establish synapses with type I_5 TGC dendrites. **A:** Low-power electron micrograph of tectal layer five from an animal in which Ipc axon terminals were anterogradely labeled and type I_5 TGC dendrites were retrogradely labeled. Five double-labeled glomerulus-like structures (G1–G5) containing labeled Ipc terminals (black arrows) and TGC dendrites (white arrows) are present in the field. **B:** High-power electron micrograph displays a DAB-labeled Ipc terminal bouton (Ipc_t) in apposition with a TGC dendritic structure labeled by the coarse deposit formed by the Ni-DAB. **C:** Labeled Ipc bouton in apposition with two labeled TGC dendritic profiles (TGC_1 and TGC_2). **D:** Labeled Ipc axon segment terminating in two boutons, one of which is contacting two labeled TGC profiles (TGC_1 and TGC_2). Note that the axon segment is packed with synaptic vesicles. Note also the postsynaptic density (asterisk) marking an asymmetric synaptic contact between the Ipc bouton and one of the TGC dendritic profiles. **E,F:** 3D reconstruction of three connected Ipc glomeruli (G1–G3) in tectal layer 5 from single-labeled material (E,F), including all the dendritic profiles (D1x–D3x) found in apposition with them (**E_1,F_1**). **G–J:** 3D reconstruction of an Ipc structure with TGC I dendritic profiles obtained from double-labeled samples. Ipc terminal in close apposition with three TGC dendritic processes (G) shown individually in H–J with the synaptic contacts reconstructed in red (S1–S3). Scale bars = 2 μm in A,E–G; 1 μm in B–D,H–J.

to the tips of the hair-like dendritic specializations (e.g., D1c, Fig. 5D,E), whereas others seemed to make contacts en passant through dendritic thickenings (e.g., D1b, D2b, Fig. 5D,E).

Tectal layer 9

The double injections of PHA-L and BDA 3k in the Ipc and Rt, respectively, also resulted in conspicuous labeled Ipc axon terminals and retrogradely labeled dendrites from neurons whose perikarya were located in layer 13 (Fig. 6A,B), including the deepest part of this layer, which contains the type II TGCs (Luksch et al., 1998; Hellmann and Güntürkün, 2001; Marín et al., 2003; Fig. 6A). However, because type I TGCs were also labeled, the band of bottlebrushes in layer 9, characteristic of the type II TGCs (Luksch et al., 1998), was obscured by the intermingled mesh of passing dendrites of type I TCGs.

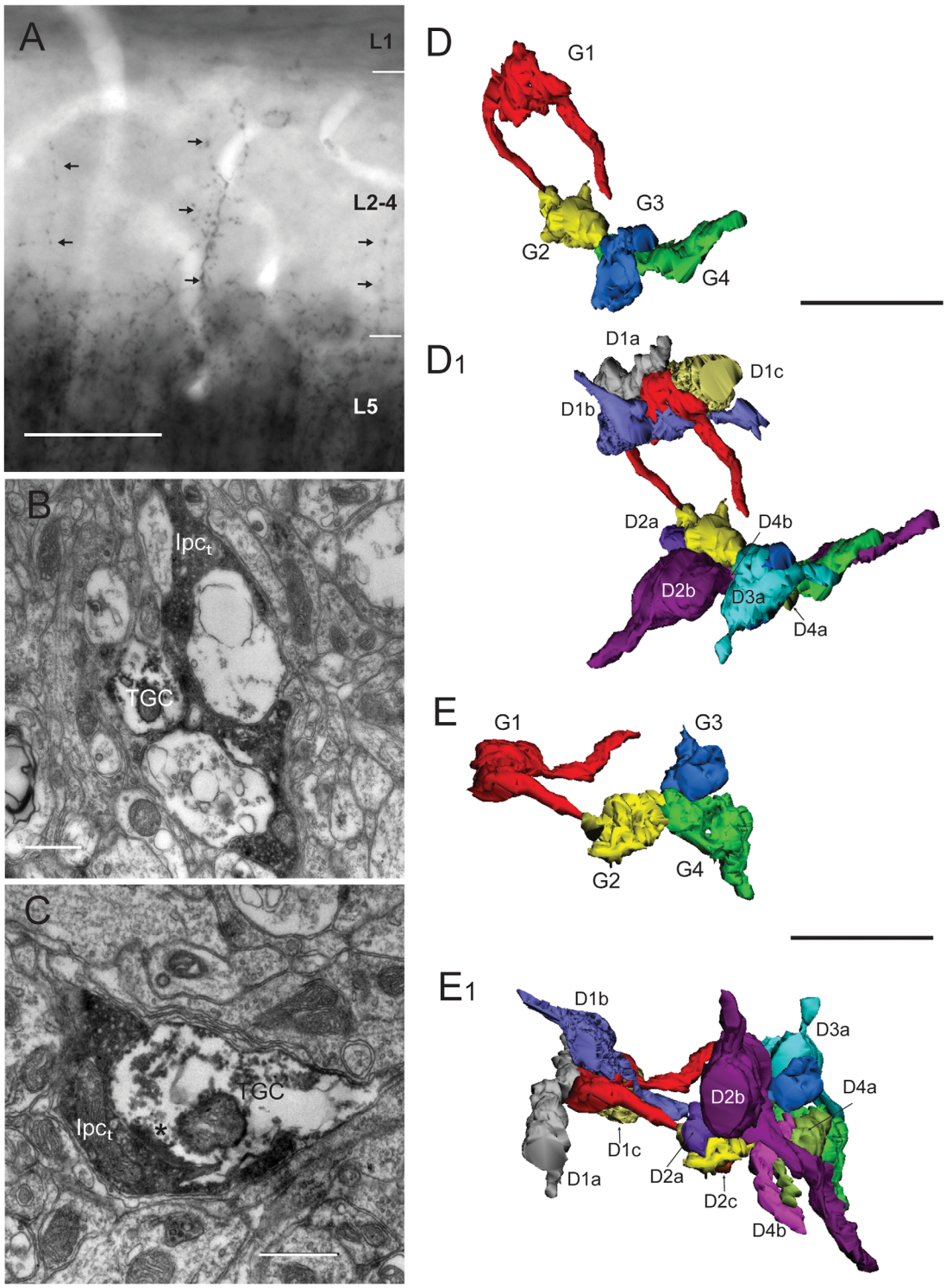

Figure 5. Ipc boutons establish synapses with type I_{2-4} TGC dendrites. **A:** Light micrograph shows labeled type I_{2-4} TGC dendritic bottlebrushes (arrows) extending beyond bottlebrushes in layer 5 reaching up to layer 2. **B:** Electron micrograph of an anterogradely labeled Ipc bouton (DAB) in apposition to a retrogradely labeled TGC dendritic profile (Ni-DAB) forming a glomerulus-like structure in tectal layers 2 and 3. **C:** Another example of a labeled Ipc bouton making synaptic contact upon a labeled TGC dendritic profile. The asterisk marks the postsynaptic density. **D,E:** 3D reconstruction of four connected Ipc glomeruli (G1–G4) in tectal layers 2 and 3 (D,E), including all the dendritic profiles (D1x-D4x) found in apposition with them (**D_1,E_1**). D and E display rotated versions of the same reconstruction. Scale bars = 50 μm in A; 0.5 μm in B,C; 2 μm in D,E. [Color figure can be viewed in the online issue, which is available at wileyonlinelibrary.com.]

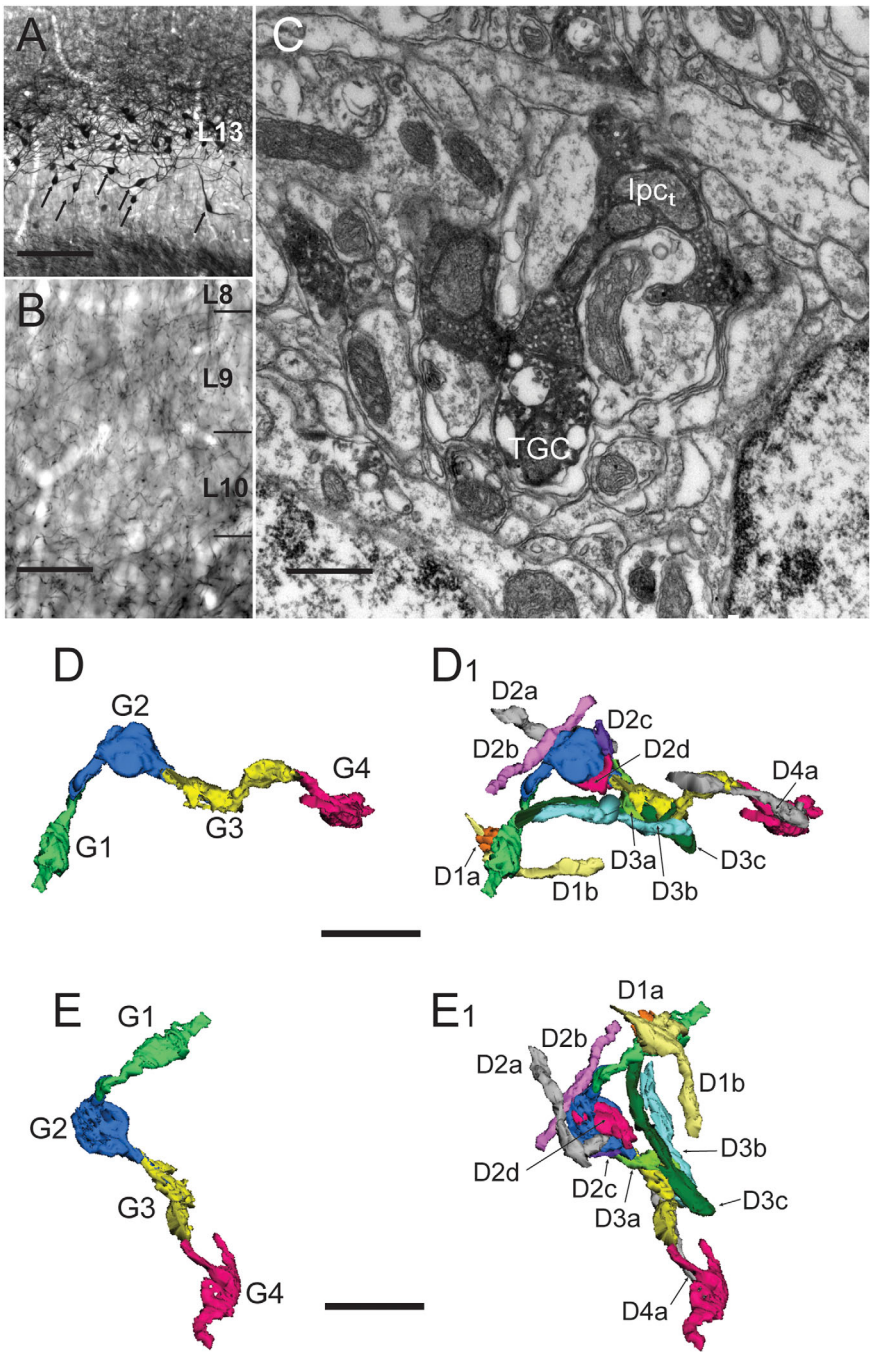

Figure 6. Ipc bouton establishes synapses with presumptive type II TGC dendrites. **A:** Light micrograph of the TeO shows retrogradely labeled TGC somata (arrows) in the deepest part of tectal layer 13, indicating the labeling of type II TGCs. **B:** Labeled dendritic processes in layer 9, possibly corresponding to type II dendritic terminations. **C:** Electron micrograph of tectal layer 9 shows an Ipc-labeled profile in apposition to a TGC dendritic profile that may correspond to a type II TGC. **D,E:** 3D reconstruction of four connected Ipc boutons (G1–G4) in tectal layer 9, including all the dendritic profiles (D1x–D4x) found in apposition with them (**D_1,E_1**). D and E display rotated versions of the same reconstruction. Scale bars = 200 μm in A; 50 μm in B; 0.5 μm in C; 2 μm in D,E. [Color figure can be viewed in the online issue, which is available at wileyonlinelibrary.com.]

In layer 9, the labeled presynaptic Ipc axonal boutons did not form prominent glomerular-like structures such as were found in the more superficial tectal layers. The Ipc boutons were seen to establish clear asymmetric synapses with unlabeled dendritic profiles and labeled dendritic profiles, presumably corresponding to type II TGCs (Fig. 6C). In single-PHA-L-labeled tissue, a single Ipc axon giving rise to four connected boutons along

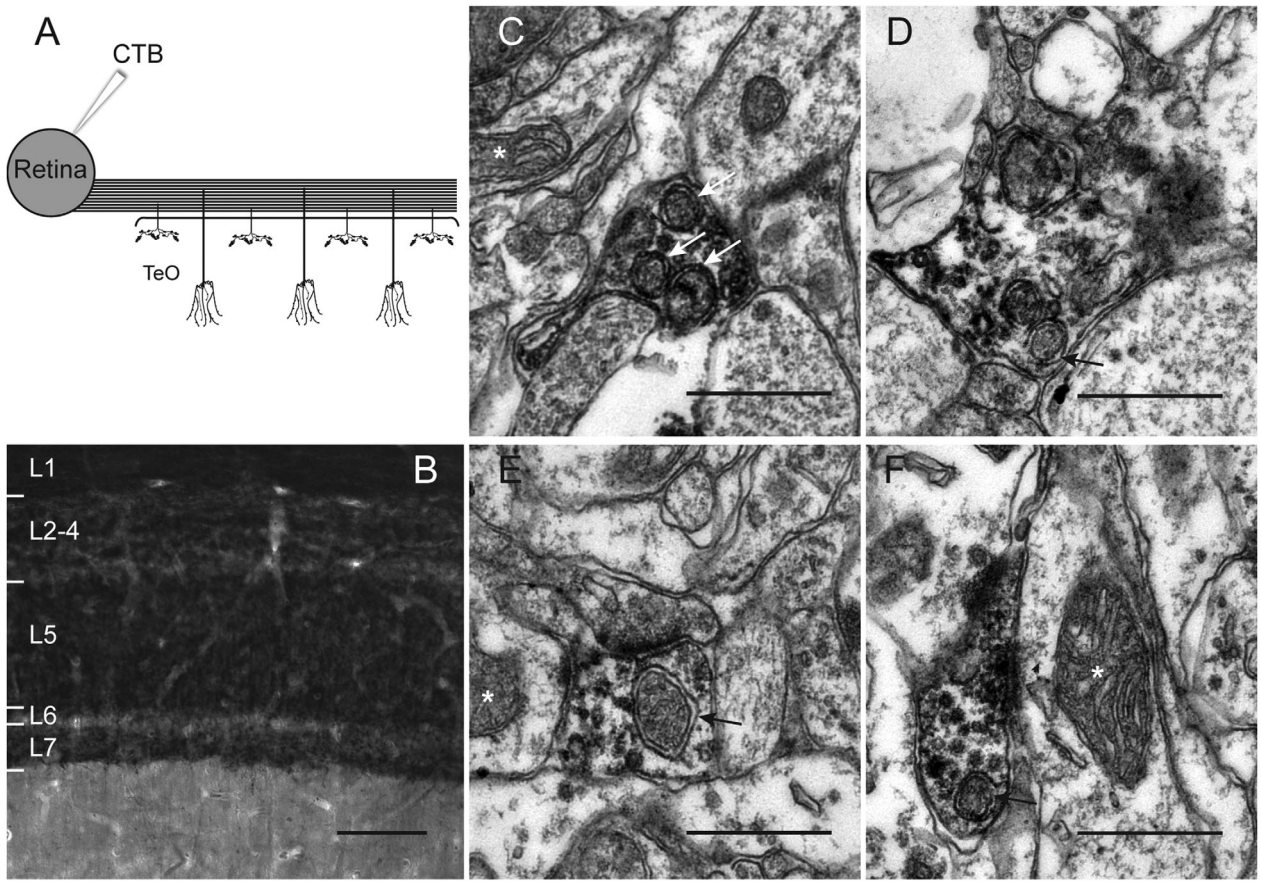

Figure 7. Mitochondria with unusually enlarged intermembrane separation identify retinal terminals in the tectum of the chicken. **A:** Schematic of the experiment with anterogradely labeled RGC terminals in the contralateral TeO. **B:** Retinorecipient layers (L1–L7) were strongly labeled after CTb injection in the contralateral eye. **C–F:** Electron micrographs from the superficial tectal layers show anterogradely labeled RGC axon terminals. These labeled profiles show the unusually enlarged mitochondria interspace (arrows) widely used by many authors (see Results) to identify retinal terminals in several vertebrates. Non-retinal profile mitochondria (asterisks) are indicated for comparison. Scale bars = 100 μm in B; 0.5 μm in C–F.

with their associated dendritic profiles was reconstructed (31 sections; Fig. 7D,E). As was found in the superficial layers, some of the dendrites contacting the Ipc boutons formed knob-like structures that terminated inside the bouton, whereas others seemed to make contacts en passant.

Synaptic analysis

As mentioned above, the Ni-DAB deposits impaired an accurate estimate of the frequency of the synaptic contacts between the Ipc boutons and the TGC dendritic processes, despite the many occasions when these contacts were clearly visualized. To quantify this synaptic interaction, we used consecutive ultrathin sections of single Ipc-labeled samples from three animals and counted the number of synapses that each Ipc bouton established with the dendritic profiles apposed to them. These analyses required 50–60 consecutive ultrathin sections for each structure studied, which included 10 and 14 glomeruli/boutons from tectal layers 2–4 and 5, respectively, and nine boutons from layer 9 (Table 3). The results showed that 94% of the dendritic profiles apposed to the Ipc boutons exhibited a clear postsynaptic density; 93% of them exhibited a single synapse, and 7% of them exhibited two synapses (Table 3). This demonstrates that the Ipc glomeruli/boutons make synaptic contact with practically all the dendrites in close apposition, which necessarily includes TGCs dendrites. Furthermore, this quantitative data revealed that the average number of dendritic profiles in apposition with labeled presynaptic Ipc boutons for the different layers investigated was two or three profiles for layers 2–4, four to six profiles for layer 5, and two or three profiles for layer 9.

Ipc/retinal ganglion cell relation

To evaluate a possible interaction between the axon terminals from the Ipc and the retinal ganglion cells

TABLE 3.
Ipc Presynaptic Profile Synaptic Analysis

Dendritic profiles	Layers 2–4 (10 boutons)	Layer 5 (14 boutons)	Layer 9 (9 boutons)	Total (33 boutons)
In apposition	21	79	22	122
Synaptic contacts	19 (90%)	75 (95%)	21 (95%)	115 (94%)
Single synapse	19 (100%[1])	67 (89%[1])	21 (100%[1])	107 (93%[1])
Two synapses		8 (11%[1])		8 (7%[1])

[1]Percentage of the total number of profiles receiving synaptic contacts.

(RGCs) in the TeO, we examined double-labeled tissue from animals that had been injected with CTb in the eye and with PHA-L in the Ipc. However, because of technical problems, it was not possible to distinguish the two types of terminals. To examine this relationship, we therefore based the identification of the RGC axon profiles in the TeO on their characteristic morphological features. These terminals tend to be moderately dark and possess mitochondria that exhibit an unusually enlarged space between the inner and outer membranes (rat, Lund, 1969; cat, Sterling, 1971; primates, Tigges et al., 1973; pigeon, Hayes and Webster, 1975). We first validated this criterion in single-labeled tissue by examining the retinorecipient tectal layers in samples obtained from animals that had received a CTb injection into the eye (Fig. 7A,B). We found that all the DAB-labeled retinal terminals examined possessed mitochondria with this characteristic feature (Fig. 7C–F).

We then examined the relationship between the Ipc and RGC axon terminals by surveying the retinorecipient tectal layers of samples from three animals that had received a PHA-L injection into the Ipc. We analyzed a total of 30 labeled Ipc glomeruli/boutons (layers 2–4 = 15 glomeruli; layer 5 = 15 glomeruli) by examining a series of consecutive ultrathin sections containing the entire structure. This analysis showed that, even though Ipc labeled profiles were found in apposition with retinal profiles, there was no evidence of synaptic connections among them.

RGC/TGC relation

We next explored whether there was a direct interaction between the retinal terminals and the TGC dendrites by using the same morphological criterion to identify the retinal terminals in samples obtained from three animals with BDA-labeled type I TGC dendrites (Fig. 8A). Labeled TGC dendrites were found in apposition to presynaptic profiles corresponding to axonal terminals of RGCs (Fig. 8B–D). Furthermore, we frequently observed several labeled TGC profiles exhibiting clear postsynaptic densities associated with the presynaptic RGC axon terminals (Fig. 8B,C), indicating a synaptic relationship between these terminals and the TGC's dendrites.

DISCUSSION

In birds and mammals, and presumably all amniotes, widefield TGCs give rise to a nontopographic, bilateral tectofugal pathway that processes and conveys visual motion signals to the thalamus (Benowitz and Karten, 1976; Robson and Hall, 1977; Luppino et al., 1988; Karten et al., 1997; Major et al., 2000; Hellmann and Güntürkün, 2001; Lyon et al., 2003; Marín et al., 2003; Chomsung et al., 2008; Day-Brown et al., 2010; Baldwin et al., 2011; Fredes et al., 2012; Gale and Murphy, 2014). In birds, the output of this pathway is controlled by a feedback projection from the Ipc nucleus (Marín et al., 2007, 2012). The present study demonstrates that Ipc axonal boutons are indeed presynaptic structures that "embed" and make synaptic contact with several dendritic profiles, some of which are TGC dendritic processes. This direct synaptic contact between the Ipc and the TGCs is likely to underlie the strong control exerted by the Ipc axons upon the tectofugal output mediated by the TGCs.

The Ipc glomerular synaptic bouton

The present study shows that the Ipc axonal boutons observed at the LM level correspond to irregular axonal profiles bounding several postsynaptic dendritic profiles. These boutons are usually wrapped together by astrocyte lamellae, thus acquiring a glomerular-like appearance. Profiles with these characteristics had been previously described in the retinorecipient tectal layers of pigeons (Hayes and Webster, 1975; Angaut and Repérant, 1976), and their origin was deemed extraretinal because they persisted after retinal terminal degeneration produced by eye removal. However, at that time, the specific source and identity of these structures were unknown.

In tectal layer 5, the Ipc boutons are packed with round and clear synaptic vesicles establishing multiple asymmetrical synapses with four to six dendritic profiles. We found that up to two of these profiles correspond to type I TGC dendritic processes. Similar

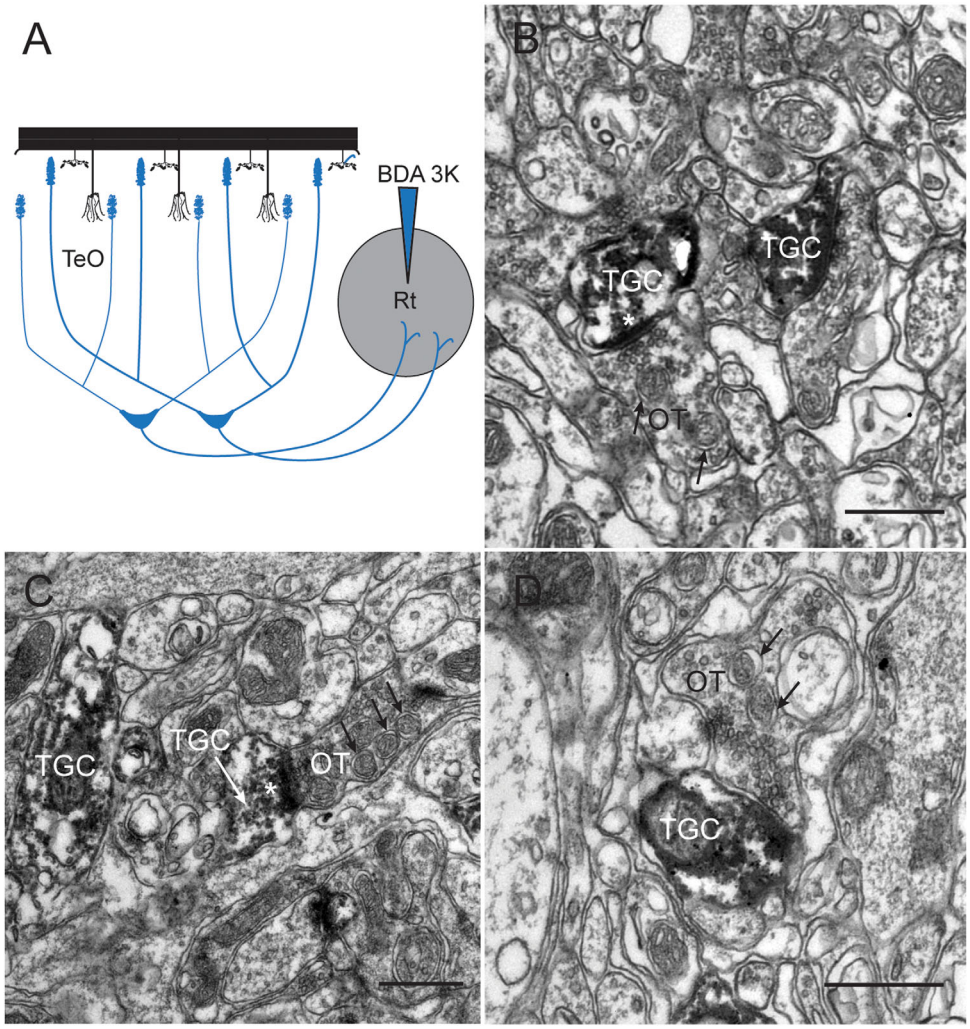

Figure 8. Retinal axon terminals establish synaptic contacts with TGC dendrites. **A:** Schematic of single BDA 3k injection in Rt to label the TGC dendrites retrogradely. **B–D:** Retrogradely labeled TGC dendritic profiles are found in apposition to retinal axon terminals (OT), identified by mitochondria featuring an enlarged intermembrane separation (arrows). The asterisks mark postsynaptic densities, indicating synaptic contacts between these structures. Scale bars = 0.5 μm. [Color figure can be viewed in the online issue, which is available at wileyonlinelibrary.com.]

structures were found in the most superficial tectal layers 2–4 and in deeper layer 9, and, as in layer 5, the boutons were loaded with synaptic vesicles embedding and making synaptic contact with two or three dendritic profiles. Some of these profiles were identified as dendritic processes from type I_{2-4} TGCs in the superficial layers and type II in the deeper layers. In the latter case, however, the paucity of both labeled TGC dendritic processes and Ipc synaptic boutons plus the eventual "contamination" of passing dendrites from other TGC types raises the possibility of misidentifications. We make this caveat despite the anatomical and physiological evidence explained below that supports such direct Ipc–type II synaptic contacts.

Our morphological analysis and 3D reconstruction of the glomerular boutons demonstrate that the Ipc axon terminals make synaptic contacts inside these structures, and, even though the interbouton axonal segments contain many synaptic vesicles, they were not seen establishing synaptic contacts. Thus, the distribution of the boutons observed by LM closely reflects the distribution of Ipc synaptic terminals across tectal layers.

By far the highest density of Ipc synaptic boutons is located in tectal layer 5, where the boutons form a dense plexus that spans the entire layer. Less dense but regularly scattered synaptic boutons stemming from parallel radial branches are observed in layers 2–4, although long branches and collateral ramifications form a third plexus of synaptic boutons around layer 9 (Wang et al., 2006). The fact that this distribution coincides with that of the dendritic specializations of the

three main types of TGC reinforces the hypothesis that the TGC dendrites are the main synaptic targets of the Ipc axons. However, the fact that usually no more than two from among three to six dendritic elements corresponded to labeled TGC processes, even in the material more heavily labeled with TGCs, indicates that the Ipc axons also make contact with other structures. Two candidates in the superficial layers are retinal axon terminals and the dendrites of the shepherd's crook neurons that convey the retinal input to the Ipc. However, in agreement with previous findings in pigeons (Hayes and Webster, 1975), we did not detect synaptic contacts between the Ipc boutons and the retinal terminals. Although functional evidence suggests an interaction between shepherd's crook neurons and Ipc axons (Marín et al., 2005), we did not detect any synaptic connections between them in the superficial layers. However, given that the dendrites of these neurons span the whole extent of the tectal layers, a synaptic contact between Ipc axons and these neurons cannot be excluded.

On the other hand, a previous article indicated that labeled Ipc axons made synaptic contacts with horizontal dendritic profiles (Hunt et al., 1977). Whether these corresponded to the TGC processes as described here or to other neural elements is unclear. Other neural processes densely represented in layer 5 are γ-aminobutyric acidergic neurites from intrinsic horizontal cells (Luksch and Golz, 2003) and neuropeptide Y-immunopositive axons from nucleus pretectalis (Gamlin and Cohen, 1988; Gamlin et al., 1996). Although axonal profiles with pleomorphic vesicles were found in layer 5, they were never observed in apposition with the Ipc bouton.

The glomerular appearance of the Ipc terminals in the superficial layers is reminiscent of the glomerular arrangement found in retinothalamic and corticothalamic connections. These synaptic complexes are characterized by large afferent glutamatergic terminals that contain packed, round synaptic vesicles (RL profiles) and make synaptic contact with several postsynaptic dendritic elements, all enclosed in a glial sheath (Famiglietti and Peters, 1972; Rapisardi and Miles, 1984; Paré and Smith, 1996; Sherman and Guillery, 2002; Li et al., 2003). The postsynaptic dendritic spines in these complexes usually emit spinules or protrusions that invaginate the terminal (Li et al., 2003; Erisir and Dreusicke, 2005). In the present study, the dendritic elements formed irregular knob-like structures that were engulfed by the Ipc terminals. Some irregularities looked like protrusions, or spinules, stemming from the knobs. However, we did not find synaptic specializations specifically associated with these thinner protrusions.

RL profiles within glomeruli are normally regarded as "drivers" in that they dominate the action of the postsynaptic neuron, in contrast to "modulators" that only modulate transmission through the postsynaptic neuron (Sherman and Guillery, 1998, 2011). In this scheme, the Ipc terminals in the chicken appear to have the morphological characteristics of a driver and would not play the modulatory role previously assumed (see below).

Ipc control of the tectofugal output

In birds, two main channels are distinguished within the TGC–Rt projection, one consisting of type I TGCs, which innervate the dorsal anterior and central subdivisions of the Rt, and the other consisting of type II TGCs, which innervate the posterior and triangularis subdivision (Karten et al., 1997; Marín et al., 2003). Subtypes of these TGCs refine this parallel connectivity (Hellmann and Güntürkün, 2001). The Ipc feedback activity seems to control all tectorotundal channels because the burst firing of Ipc axons induces a synchronic firing in neurons across the rotundus. Likewise, blocking the Ipc feedback in a tectal locus prevents visual responses from that locus in all rotundal subdivisions (Marín et al., 2012). The asymmetric synapses between the Ipc terminal boutons and the dendrites of type I TGCs and, apparently, also the type II TGCs would be the anatomical substrate of this cross-channel control (Fig. 9).

It is generally accepted that the tectal modulation by the isthmi is cholinergic because the Ipc and its presumptive homologues in other vertebrates are immunopositive for choline acetyltransferase; indeed, one proposed mechanism of Ipc control over tectofugal output is presynaptic facilitation of retinotectal synapses mediated by acetylcholine. In amphibians, isthmic stimulation produces depolarization of retinal terminals (Dudkin and Gruberg, 2003). However, we did not find synaptic contacts between the Ipc boutons and the retinal terminals, and Ipc neurons in the chicken do not express or express very low levels of the mRNA coding for the vesicular acetylcholine transporter (González-Cabrera et al., 2015). Instead, they strongly express vesicular glutamate transporter 2 mRNA (Islam and Atoji, 2008; González-Cabrera et al., 2015) and the corresponding protein in their terminals (González-Cabrera et al., 2015), strongly suggesting that they use glutamate as a transmitter. Thus, although Ipc terminals in the chicken may release acetylcholine through a nonvesicular mechanism (Israël et al., 1986, 1994; Bloc et al., 1999, 2000; Chávez et al., 2011) and exert a paracrine influence on retinal terminals, the neurochemical and morphological characteristics of the Ipc synaptic terminals support a direct driving effect on the TGC

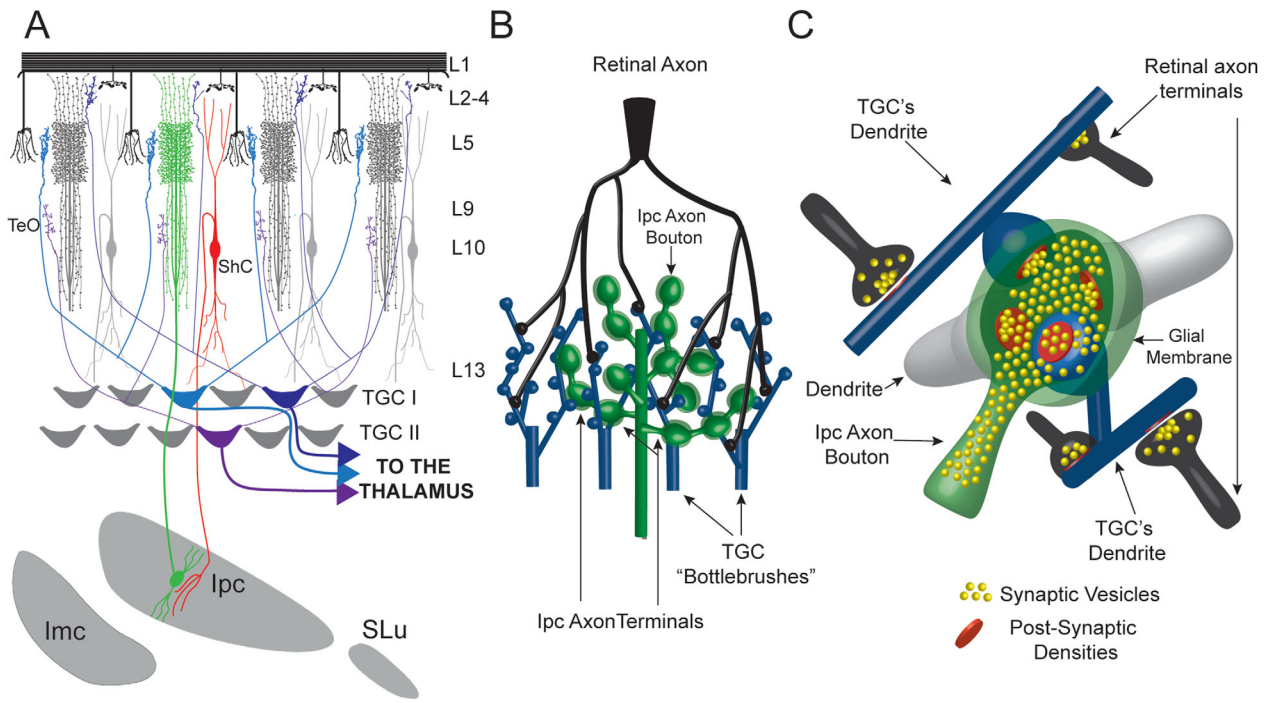

Figure 9. Summary of the Ipc–TGC synaptic organization. **A:** Schematic of retina–isthmotectal connectivity. Tectal shepherd's crook (ShC; red) cells project to the isthmic complex. The Ipc axons (green) feed back onto the tectum, each spreading hundreds of boutons in the superficial and deep layers of the tectum. The retinal terminals make synaptic contacts with the dendrites of the type I_5 (light blue) and type I_{2-4} (blue) TGCs. The Ipc boutons make synaptic contacts with different types of TGC dendrites (types I_5, I_{2-4}, and II; purple), explaining the strong control exerted by these axons over the visual activity in the thalamic Rt. **B:** Enlarged schematic shows a detailed view of the TGC bottlebrushes (blue) establishing synaptic contact with an Ipc axon terminal branch (green) and a retinal axon terminal (black) in the superficial TeO. **C:** Schematic of a single Ipc glomerulus formed by an Ipc bouton (green) filled with synaptic vesicles (yellow). This Ipc bouton establishes asymmetric synapses (red) with several dendritic profiles (white and blue). At least two of these dendrites correspond to TGC dendrites (blue). These components are wrapped by glial membrane (light green). TGC dendrites also receive asymmetric synapses from RGC axonal terminal (black) outside the glomerulus.

dendrites, presumably mediated by glutamate. Electrophysiological evidence suggests that the long dendrites of the TGCs transmit action potentials (birds, Luksch et al., 2001; mouse, Gale and Murphy, 2014), which suggests that the retinal postsynaptic potentials must overcome a threshold at the dendritic brush-like terminal to trigger and to transmit an impulse to the soma. It is possible that the glutamate liberated by the retinal terminal produces a subthreshold depolarization on the dendritic processes that is overcome when pulses of glutamate are released by the Ipc terminal. This mechanism would underlie both the gating effect and the rhythmic firing imposed by the Ipc feedback on the tectofugal output (for a similar mechanism in the fly, see Huston and Krapp, 2009).

Implications of the present findings for TGC studies in other amniotes

The TGC-mediated tectofugal pathway transmitting visual motion signals to the thalamus and thence to the pallium is highly conserved in all amniotes. The function of this pathway remains unclear, but its conserved character underlies its functional relevance. From a functional point of view, the most conspicuous characteristic of TGC neurons is their motion sensitivity (Humphrey, 1968; Schmidt and Bischof, 2001; Wu et al., 2005; Gale and Murphy, 2014), especially to small moving targets and looming stimuli, and their bilateral, nontopographic projection to the thalamus. The fact that in birds these neurons are tightly controlled by a competitive spatial mechanism raises the question of whether an analogous mechanism exists in the other amniotes. The nontopographic characteristic of the TGC–thalamic projection may require such a selective spatial filter, given that thalamic neurons would be saturated by neural activity evoked by multiple visual objects. In pigeons, the Ipc bursting feedback both gates the most salient visual signals with topographic precision and imprints a rhythm onto the transmitted visual input such that the Rt activity across the Rt becomes synchronized to the Ipc feedback, which, perhaps,

"tags" in this way the selected visual activity (Marín et al., 2012). In reptiles, the isthmotectal circuit seems identical to that of birds and presumably has a similar function (Sereno and Ulinski, 1987). In mammals, the nucleus parabigeminus (PBN) is the presumptive homologue of the Ipc nucleus (Graybiel, 1978; Mufson et al., 1986; Diamond et al., 1992; Cui and Malpeli, 2003), and evidence indicates that its activity is related to attention and stimulus selection during visual tracking (Ma et al., 2013); thus, its functional relationship with the TGCs deserves investigation at the anatomical and physiological levels. Alternatively, the visual cortex may have taken over the gating process. In the mouse, the visual cortex projects directly to the TGCs (S. Gale and G. Murphy, personal communication), and looming-sensitive neurons from the colliculus, presumptive TGCs, decrease their gain response by up to 50% when the visual cortex is selectively inactivated (Zhao et al., 2014). In birds, layer 13 neurons also receive the projection from prominent telencephalic visual centers, the visual Wulst (Karten et al., 1973; Miceli et al., 1987) and the arcopallium (Zeir and Karten 1971; Knudsen et al., 1995; Davies et al., 1997; Dubbeldam et al., 1997), and evidence for the owl suggests that the arcopallium modulates the competition among active layer 13 neurons via the isthmotectal circuitry (Mysore and Knudsen, 2013, 2014). An additional possibility is that intrinsic collicular feedback connections (Ghitani et al., 2014) might control the TGC output in the mouse.

In conclusion, the present work shows that Ipc axon terminals are organized at a tectal level in glomerulus-like structures, establishing synaptic relationships with TGC dendrites in tectal layers 2–4 and 5 and, presumably, in layer 9 as well. This suggests that Ipc control over TGC visual outflow is by direct synaptic contact. In mammals, the PBN, visual cortex, or intrinsic collicular circuits might exert an analogous control.

ACKNOWLEDGMENTS

The authors thank Prof. Juan Fernandez for his invaluable scientific advice, Mr. Solano Henriquez and Mr. Gareth Hazell for their helpful technical support, and Mr. Christian Morales for his scientific assistance.

CONFLICT OF INTEREST STATEMENT

The authors declare that they have no conflicts of interest.

ROLE OF AUTHORS

All authors had full access to all the data in the study and take responsibility for the integrity of the data and the accuracy of the data analysis. Study concept and design: CG-C, JM, JPB, GJM. Acquisition of data: CG-C, FG-C, GJM. Analysis and interpretation of data: CG-C, FG-C, JM, JPB, GJM. Drafting of the manuscript: CG-C, FG-C, JPB, GJM. Critical revision of the article for important intellectual content: CG-C, FG-C, JPB, GJM. Statistical analysis: CG-C, FG-C. Obtained funding: GJM, JPB. Study supervision: JPB, GJM.

LITERATURE CITED

Angaut P, Repérant J. 1976. Fine structure of the optic fibre termination in the pigeon optic tectum: a Golgi and electron microscope study. Neuroscience 1:93–105.

Baldwin MKL, Wong P, Reed JL, Kaas JH. 2011. Superior colliculus connections with visual thalamus in gray squirrels (*Sciurus carolinensis*): evidence for four subdivisions within the pulvinar complex. J Comp Neurol 519:1071–1094.

Benowitz LI, Karten HJ. 1976. Organization of the tectofugal visual pathway in the pigeon: a retrograde transport study. J Comp Neurol 167:503–520.

Bloc A, Bugnard E, Dunant Y, Falk-Vairant J, Israël M, Loctin F, Roulet E. 1999. Acetylcholine synthesis and quantal release reconstituted by transfection of mediatophore and choline acetyltranferase cDNAs. Eur J Neurosci 11: 1523–1534.

Bloc A, Bancila V, Israël M, Dunant Y. 2000. Reconstitution of mediatophore-supported quantal acetylcholine release. Metab Brain Dis 15:1–16.

Chávez J, Vargas MH, Cruz-Valderrama JE, Montaño LM. 2011. Nonquantal release of acetylcholine in guinea pig airways: role of choline transporter. Exp Physiol 96:460–467.

Chomsung RD, Petry HM, Bickford ME. 2008. Ultrastructural examination of diffuse and specific tectopulvinar projections in the tree shrew. J Comp Neurol 510:24–46.

Comoli E, Das Neves Favaro P, Vautrelle N, Leriche M, Overton PG, Redgrave P. 2012. Segregated anatomical input to subregions of the rodent superior colliculus associated with approach and defense. Front Neuroanat 6:9.

Cui H, Malpeli JG. 2003. Activity in the parabigeminal nucleus during eye movements directed at moving and stationary targets. J Neurophysiol 89:3128–3142.

Davies DC, Csillag A, Székely AD, Kabai P. 1997. Efferent connections of the domestic chick archistriatum: a *Phaseolus* lectin anterograde tracing study. J Comp Neurol 389: 679–693.

Day-Brown JD, Wei H, Chomsung RD, Petry HM, Bickford ME. 2010. Pulvinar projections to the striatum and amygdala in the tree shrew. Front Neuroanat 4:143.

Diamond IT, Fitzpatrick D, Conley M. 1992. A projection from the parabigeminal nucleus to the pulvinar nucleus in Galago. J Comp Neurol 316:375–382.

Dubbeldam JL, Den Boer-Visser AM, Bout RG. 1997. Organization and efferent connections of the archistriatum of the nallard, *Anas platyrhynchos* L.: an anterograde and retrograde tracing study. J Comp Neurol 388:632–657.

Dudkin E, Gruberg E. 2003. Nucleus isthmi enhances calcium influx into optic nerve fiber terminals in *Rana pipiens*. Brain Res 969:44–52.

Erisir A, Dreusicke M. 2005. Quantitative morphology and postsynaptic targets of thalamocortical axons in critical period and adult ferret visual cortex. J Comp Neurol 485:11–31.

Famiglietti EV, Peters A. 1972. The synaptic glomerulus and the intrinsic neuron in the dorsal lateral geniculate nucleus of the cat. J Comp Neurol 144:285–334.

Fredes F, Vega-Zuniga T, Karten H, Mpodozis J. 2012. Bilateral and ipsilateral ascending tectopulvinar pathways in mammals: a study in the squirrel (*Spermophilus beecheyi*). J Comp Neurol 520:1800–1818.

Gale SD, Murphy GJ. 2014. Distinct representation and distribution of visual information by specific cell types in mouse superficial superior colliculus. J Neurosci 34: 13458–13471.

Gamlin PDR, Cohen DH. 1988. Projections of the retinorecipient pretectal nuclei in the pigeon (*Columba livia*). J Comp Neurol 269:18–46.

Gamlin PDR, Reiner A, Keyser KT, Brecha N, Karten HJ. 1996. Projection of nucleus pretectalis to a retinorecipient tectal layer in the pigeon (*Columba livia*). J Comp Neurol 368:424–438.

Gandhi NJ, Katnani HA. 2011. Motor functions of the superior colliculus. Annu Rev Neurosci 34:205–231.

Ghitani N, Bayguinov PO, Vokoun CR, McMahon S, Jackson MB, Basso MA. 2014. Excitatory synaptic feedback from the motor layer to the sensory layers of the superior colliculus. J Neurosci 34:6822–6833.

González-Cabrera C, Garrido-Charad F, Roth A, Marín GJ. 2015. The isthmic nuclei providing parallel feedback connections to the avian tectum have different neurochemical identities: expression of glutamatergic and cholinergic markers in the chick (*Gallus gallus*). J Comp Neurol 523:1341–1358.

Graybiel AM. 1978. A satellite system of the superior colliculus: the parabigeminal nucleus and its projections to the superficial collicular layers. Brain Res 145:365–374.

Gruberg E, Dudkin E, Wang Y, Marín G, Salas C, Sentis E, Letelier J, Mpodozis J, Malpeli J, Cui H, Ma R, Northmore D, Udin S. 2006. Influencing and interpreting visual input: the role of a visual feedback system. J Neurosci 26:10368–10371.

Güntürkün O, Remy, M. 1990. The topographical projection of the nucleus isthmi pars parvocellularis (Ipc) onto the tectum opticum in the pigeon. Neurosci Lett 111:18–22.

Hayes BP, Webster KE. 1975. An electron microscope study of the retinoreceptive layers of the pigeon optic tectum. J Comp Neurol 162:447–466.

Hellmann B, Güntürkün O. 2001. Structural organization of parallel information processing within the tectofugal visual system of the pigeon. J Comp Neurol 429:94–112.

Humphrey NK. 1968. Responses to visual stimuli of units in the superior colliculus of rats and monkeys. Exp Neurol 20:312–340.

Hunt SP, Streit P, Künzle H, Cuénod M. 1977. Characterization of the pigeon isthmotectal pathway by selective uptake and retrograde movement of radioactive compounds and by Golgi-like horseradish peroxidase labeling. Brain Res 129:197–212.

Huston SJ, Krapp HG. 2009. Nonlinear integration of visual and haltere inputs in fly neck motor neurons. J Neurosci 29:13097–13105.

Ingle DJ. 1983. Brain mechanisms of visual localization by frogs and toads. In: Ewert J-P, Capranica RR, Ingle DJ, editors. Advances in vertebrate neuroethology. NATO Advanced Science Institutes Series, volume 56. New York: Springer. p 177–226.

Islam MR, Atoji Y. 2008. Distribution of vesicular glutamate transporter 2 and glutamate receptor 1 mRNA in the central nervous system of the pigeon (*Columba livia*). J Comp Neurol 511:658–677.

Israël M, Morel N, Lesbats B, Birman S, Manaranche R. 1986. Purification of a presynaptic membrane protein that mediates a calcium-dependent translocation of acetylcholine. Proc Natl Acad Sci U S A 83:9226–9230.

Israël M, Lesbats B, Synguelakis M, Joliot A. 1994. Acetylcholine accumulation and release by hybrid NG108-15, glioma, and neuroblastoma cells—role of a 16 kDa membrane protein in release. Neurochem Int 25:103–109.

Karten HJ, Hodos W, Nauta WJH, Revzin AM. 1973. Neural connections of the "visual wulst" of the avian telencephalon. Experimental studies in the pigeon (*Columba livia*) and owl (*Speoiyto cunicularia*). J Comp Neurol 150:253–278.

Karten HJ, Cox K, Mpodozis J. 1997. Two distinct populations of tectal neurons have unique connections within the retinotectorotundal pathway of the pigeon (*Columba livia*). J Comp Neurol 387:449–465.

Knudsen EI, Cohen YE, Masino T. 1995. Characterization of a forebrain gaze field in the archistratum of the brain owl. Microstimulation and anatomical connections. J Neurosci 15:5139–5151.

Krauzlis RJ, Lovejoy LP, Zénon A. 2013. Superior colliculus and visual spatial attention. Annu Rev Neurosci 36:165–182.

Li J, Wang S, Bickford ME. 2003. Comparison of the ultrastructure of cortical and retinal terminals in the rat dorsal lateral geniculate and lateral posterior nuclei. J Comp Neurol 460:394–409.

Luksch H, Golz S. 2003. In vivo electrophysiological and anatomical characterization of GABAergic subpopulations in the ventral tegmental area (VTA) of adult mice. J Chem Neuroanat 25:185–194.

Luksch H, Cox K, Karten HJ. 1998. Bottlebrush dendritic endings and large dendritic fields: motion-detecting neurons in the tectofugal pathway. J Comp Neurol 396:399–414.

Luksch H, Karten HJ, Kleinfeld D, Wessel R. 2001. Chattering and differential signal processing in identified motion-sensitive neurons of parallel visual pathways in the chick tectum. J Neurosci 21:6440–6446.

Lund RD. 1969. Synaptic patterns of the superficial layers of the superior colliculus of the rat. J Comp Neurol 135: 179–208.

Luppino G, Matelli M, Carey RG, Fitzpatrick D, Diamond IT. 1988. New view of the organization of the pulvinar nucleus in *Tupaia* as revealed by tectopulvinar and pulvinar-cortical projections. J Comp Neurol 273:67–86.

Lyon DC, Jain N, Kaas JH. 2003. The visual pulvinar in tree shrews I. Multiple subdivisions revealed through acetylcholinesterase and Cat-301 chemoarchitecture. J Comp Neurol 467:593–606.

Ma R, Cui H, Lee S-H, Anastasio TJ, Malpeli JG. 2013. Predictive encoding of moving target trajectory by neurons in the parabigeminal nucleus. J Neurophysiol 109:2029–2043.

Major DE, Luksch H, Karten HJ. 2000. Bottlebrush dendritic endings and large dendritic fields: motion-detecting neurons in the mammalian tectum. J Comp Neurol 423:243–260.

Marín G, Letelier JC, Henny P, Sentis E, Farfán G, Fredes F, Pohl N, Karten H, Mpodozis J. 2003. Spatial organization of the pigeon tectorotundal pathway: an interdigitating topographic arrangement. J Comp Neurol 458:361–380.

Marín G, Mpodozis J, Sentis E, Ossandon T, Letelier JC. 2005. Oscillatory bursts in the optic tectum of birds represent re-entrant signals from the nucleus isthmi pars parvocellularis. J Neurosci 25:7081–7089.

Marín G, Salas C, Sentis E, Rojas X, Letelier JC, Mpodozis J. 2007. A cholinergic gating mechanism controlled by competitive interactions in the optic tectum of the pigeon. J Neurosci 27:8112–8121.

Marín G, Duran E, Morales C, González-Cabrera C, Sentis E, Mpodozis J, Letelier JC. 2012. Attentional capture? Synchronized feedback signals from the isthmi boost retinal signals to higher visual areas. J Neurosci 32:1110–1122.

May PJ. 2006. The mammalian superior colliculus: laminar structure and connections. Prog Brain Res 151:321–378.

Miceli D, Repérant J, Villalobos J, Dionne L. 1987. Extratelencephalic projections of the avian visual Wulst. A quantitative autoradiographic study in the pigeon *Columbia livia*. J Hirnforsch 28:45–57.

Mufson EJ, Martin TL, Mash DC, Wainer BH, Mesulam MM. 1986. Cholinergic projections from the parabigeminal nucleus (Ch8) to the superior colliculus in the mouse: a combined analysis of horseradish peroxidase transport and choline acetyltransferase immunohistochemistry. Brain Res 370:144–148.

Mysore SP, Knudsen EI. 2011. The role of a midbrain network in competitive stimulus selection. Curr Opin Neurobiol 21:653–660.

Mysore SP, Knudsen EI. 2013. A shared inhibitory circuit for both exogenous and endogenous control of stimulus selection. Nat Neurosci 16:473–478.

Mysore SP, Knudsen EI. 2014. Descending control of neural bias and selectivity in a spatial attention network: rules and mechanisms. Neuron 84:214–226.

Paré D, Smith Y. 1996. Thalamic collaterals of corticostriatal axons: their termination field and synaptic targets in cats. J Comp Neurol 372:551–567.

Peters A, Palay S, Webster H. 1991. The fine structure of the nervous system. New York: Oxford University Press.

Rapisardi SC, Miles TP. 1984. Synaptology of retinal terminals in the dorsal lateral geniculate nucleus of the cat. J Comp Neurol 223:515–524.

Robson JA, Hall WC. 1977. The organization of the pulvinar in the grey squirrel (*Sciurus carolinensis*). I. Cytoarchitecture and connections. J Comp Neurol 173:355–388.

Schmidt A, Bischof HJ. 2001. Neurons with complex receptive fields in the stratum griseum centrale of the zebra finch (*Taeniopygia guttata castanotis* Gould) optic tectum. J Comp Physiol A 187:913–924.

Sereno MI, Ulinski PS. 1987. Caudal topographic nucleus isthmi and the rostral nontopographic nucleus isthmi in the turtle, *Pseudemys scripta*. J Comp Neurol 261:319–346.

Sherman SM, Guillery RW. 1998. On the actions that one nerve cell can have on another: distinguishing "drivers" from "modulators." Proc Natl Acad Sci U S A 95:7121–7126.

Sherman SM, Guillery RW. 2002. The role of the thalamus in the flow of information to the cortex. Philos Trans R Soc Lond B Biol Sci 357:1695–1708.

Sherman SM, Guillery RW. 2011. Distinct functions for direct and transthalamic corticocortical connections. J Neurophysiol 106:1068–1077.

Sridharan D, Knudsen EI. 2014. Gamma oscillations in the midbrain spatial attention network: linking circuits to function. Curr Opin Neurobiol 31:189–198.

Sterling P. 1971. Receptive fields and synaptic organisation of the superficial grey layer of the cat superior colliculus. Vision Res 3(Suppl):309–329.

Tigges M, Tigges J, Luttrell GL, Frazier CM. 1973. Ultrastructural changes in the superficial layers of the superior colliculus in *Galago crassicaudatus* (primates) after eye enucleation. Z Zellforsch Mikrosk Anat 140:291–307.

Wang Y, Luksch H, Brecha NC, Karten HJ. 2006. Columnar projections from the cholinergic nucleus isthmi to the optic tectum in chicks (*Gallus gallus*): a possible substrate for synchronizing tectal channels. J Comp Neurol 494:7–35.

Wu LQ, Niu YQ, Yang J, Wang SR. 2005. Tectal neurons signal impending collision of looming objects in the pigeon. Eur J Neurosci 22:2325–2331.

Wylie DR, Gutierrez-Ibanez C, Pakan JM, Iwaniuk AN. 2009. The optic tectum of birds: mapping our way to understanding visual processing. Can J Exp Psychol 63:328–338.

Zeier H, Karten HJ. 1971. The archistriatum of the pigeon: organization of afferent and efferent connections. Brain Res 31:313–326.

Zhao X, Liu M, Cang J. 2014. Visual cortex modulates the magnitude but not the selectivity of looming-evoked responses in the superior colliculus of awake mice. Neuron 84:202–213.